Non-centrosymmetric features in nanostructured MoS_2 and WS_2 exfoliated in liquid phase: Supporting information

Gabriel Cardenas-Chirivi,[†] Cristina Navarrete,[†] Diana Lozano,[†] Cesar Herreño,[‡] and Yenny Hernandez[*,†]

†*Department of Physics, Universidad de los Andes, 111711, Bogotá, Colombia*

‡*Department of Science and Education, Universidad Distrital Francisco José de Caldas, 11021-110231588, Bogotá, Colombia*

E-mail: yr.hernandez@uniandes.edu.co

Sample preparation protocol

Time parameters for each process on the exfoliation protocol were evaluated extensively by fabricating all possible suspensions as an experimental design scheme. Best dispersions were obtained by the protocol in Fig. S1.

Figure S1: Liquid Phase exfoliation process for TMDs. (a) MoS_2 or WS_2 powder added to solution. (b) Ultrasonic bath with temperature control. (c) Ultrasonic tip with temperature control. (d) Filtering and cleaning of the solvent NMP. (e)Redispersion on deionized H_2O. (f) Centrifugation to ensure phases separation. (g) Selection of the 70% less weighted traces. (h) Peak analysis by UV-VIS Spectroscopy.

UV-VIS spectroscopy

Position of excitonic modes for best dispersions were compared with references of CVD and mechanical exfoliated monolayers as exhibited in Table 1.

Table 1: Excitonic modes of MoS_2 and WS_2. Reports to compare bulk, exfoliated and growth techniques

A[nm]	B[nm]	C[nm]	MoS_2	WS_2	1L	Bulk	LPE	Ref.
660	605		x		x			[1]
652	607		x		x			[2]
692	634		x			x		[3]
681	616		x			x		[4]
663	613		x		x			[5]
613	518			x	x			[2]
613	515			x	x			[6]
630	528	456		x		x		[7]
628	525	424		x			x	[8]
670	610	450	x				x	[8]
692	639	571	x			x		this study
684	624	495	x				x	this study
637	533	460		x		x		this study
626	533	465		x			x	this study

Tauc plots were conducted to find band-gap energy, using accurate parameter of order $r = 2$ for indirect transition corresponding to bulk suspension and $r = 1/2$ for direct transition for LPE version. Fig. S2 shows extrapolation curves cutting energy axes at $\sim$1.12 eV and $\sim$1.43 eV for MoS_2 bulk and nanostructure, respectively. On its side, for WS_2 $\sim$1.28 eV and $\sim$1.92 eV showing smaller values for both bulk materials than for the respective nanostructure corresponding with the expectations.

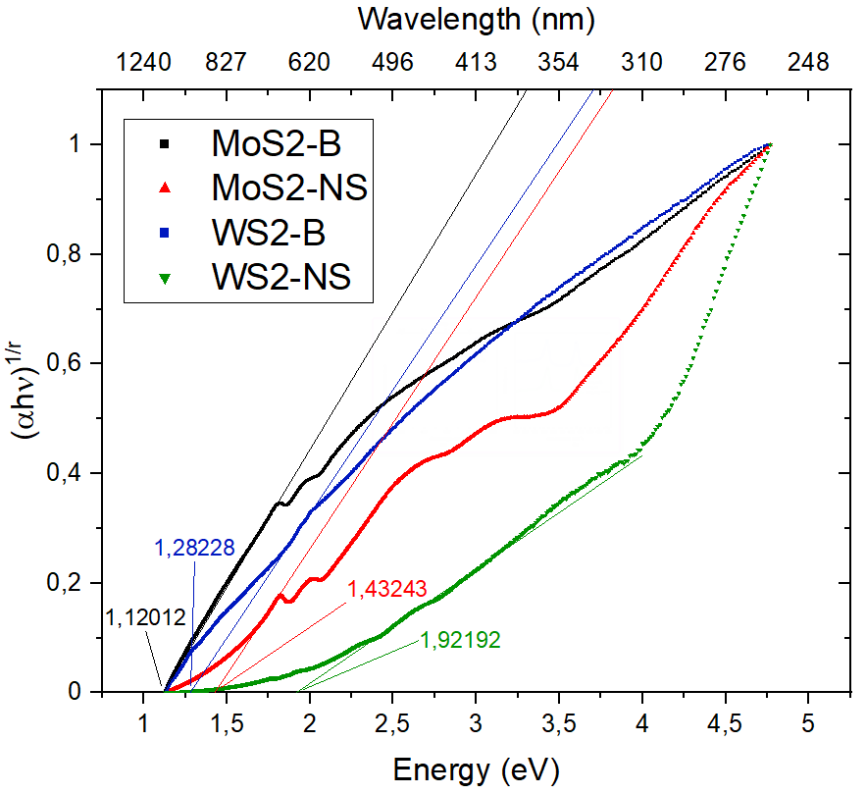

Figure S2: Tauc plot of LPE samples UV-VIS spectroscopy of MoS_2 and WS_2.

AFM histograms and monolayers

Black lines in AFM tapping-mode images Fig. S3, show standard population of flakes, analyzed to produce heights and lengths histograms. Height histograms exposed in principal document as number of layers were obtained by dividing heights over 0.65 nm and 1.01 nm for MoS_2 and WS_2, respectively. Lengths distribution in Fig. S4 show different tendency among both materials, it exhibits that optimized process made for MoS_2 results in different distribution of sizes and lengths when used for WS_2 exfoliation. Mean size of MoS_2 stands on 150nm while for WS_2 is 200nm with a greater dispersion.

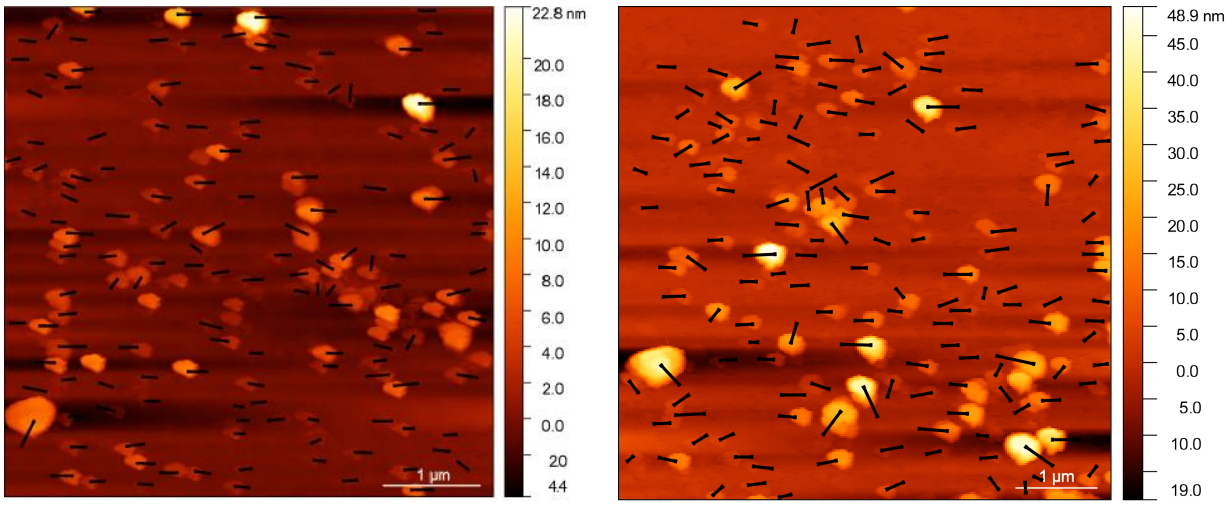

Figure S3: Representation of flakes analyzed throught AFM tapping-mode. On left side, 141 lines for MoS_2 flakes. On right side, 151 lines for WS_2 flakes.

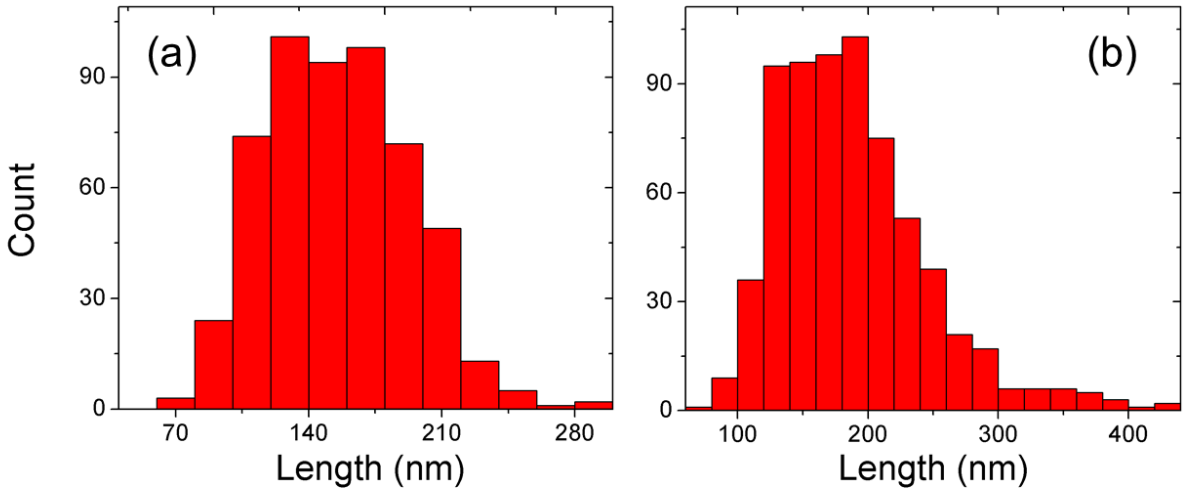

Figure S4: Histograms for length of (a) MoS_2 and (b) WS_2 flakes visualized on Fig S3.

TMD monolayers

In Fig. S5, MoS_2 and WS_2 nanostructures and monolayers are analyzed individually by SEM and AFM measurements. Results are discussed in the main manuscript.

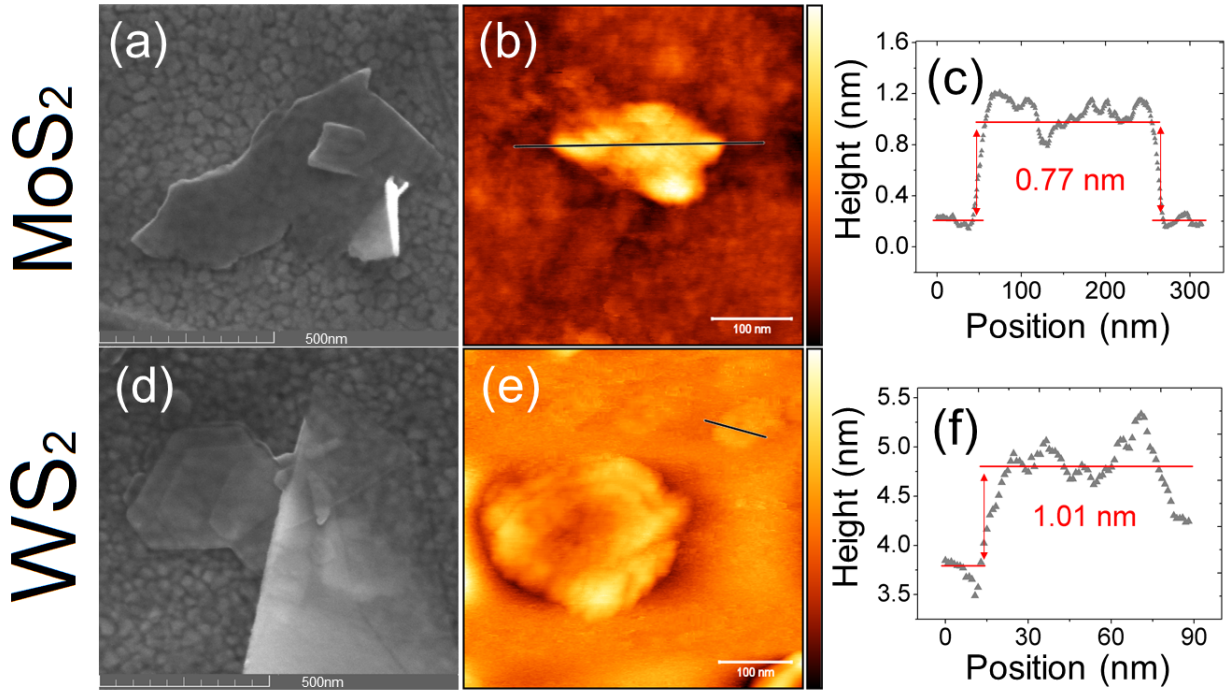

Figure S5: (a) SEM, (b) AFM and (c) profile analysis of a single flake of MoS_2 LFE. (d) SEM, (e) AFM, (f) profile analysis of WS_2 LPE. SEM samples were deposited over substrates of SiO_2 covered with 100 nm of Au while AFM samples were deposited over substrates of Si.

PFM analysis

An SS-PFM analysis was done over MoS_2 and the substrate. This is to confirm that the piezoresponse measured in DART-PFM is not associated with electrostatic or flexoelectric artifacts due to scanning sample surface. Piezoresponse results are summarized in Fig. S6 and are discussed in the main manuscript.

On the other hand, in Fig. S7, WS_2 nanoflakes are analyzed by DART-PFM and SS-PFM analysis. Results are discussed in the main manuscript.

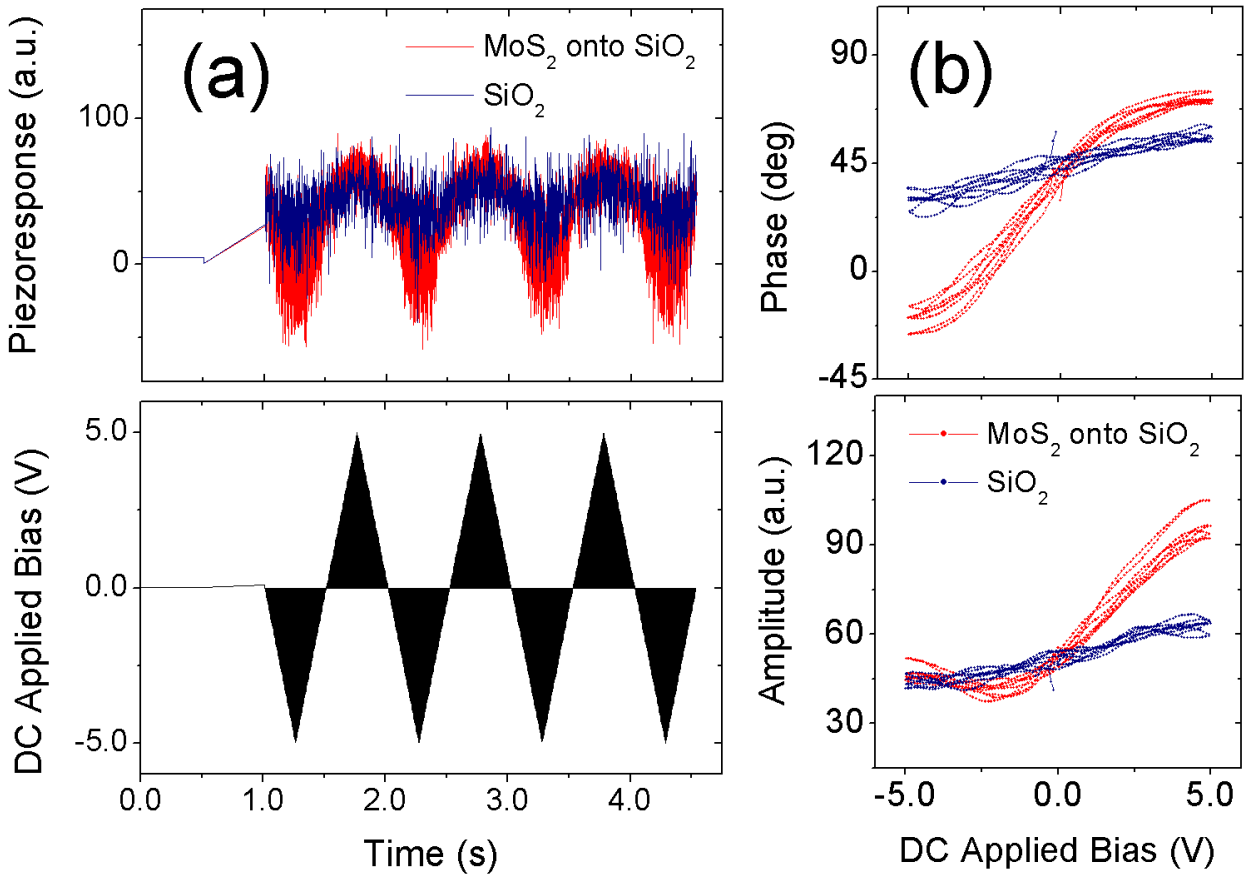

Figure S6: SS-PFM analysis in MoS_2 onto 300 nm SiO_2/Si substrates. (a) Piezoresponse and DC pulses over time. (b) Piezoresponse phase and amplitude in function of DC applied bias.

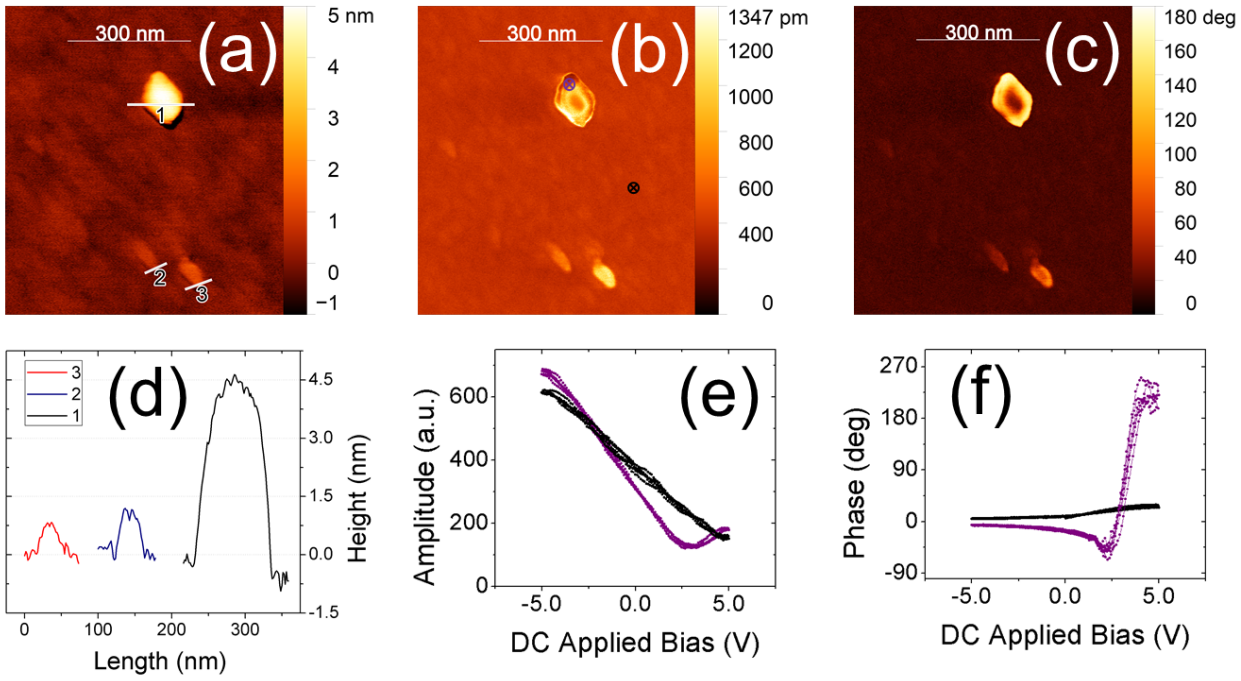

Figure S7: DART-PFM and SS-PFM analysis of WS_2 exfoliated onto 300 nm SiO_2/Si substrate. (a) Contact-mode topography. DART-PFM piezoresponse (b) amplitude and (c) phase. (d) Height profiles of nanoflakes in (a). SS-PFM piezoresponse (e) amplitude and (f) phase in function of DC applied bias. Marked points in (b) represent places where SS-PFM measurements were done.

Fluorescence

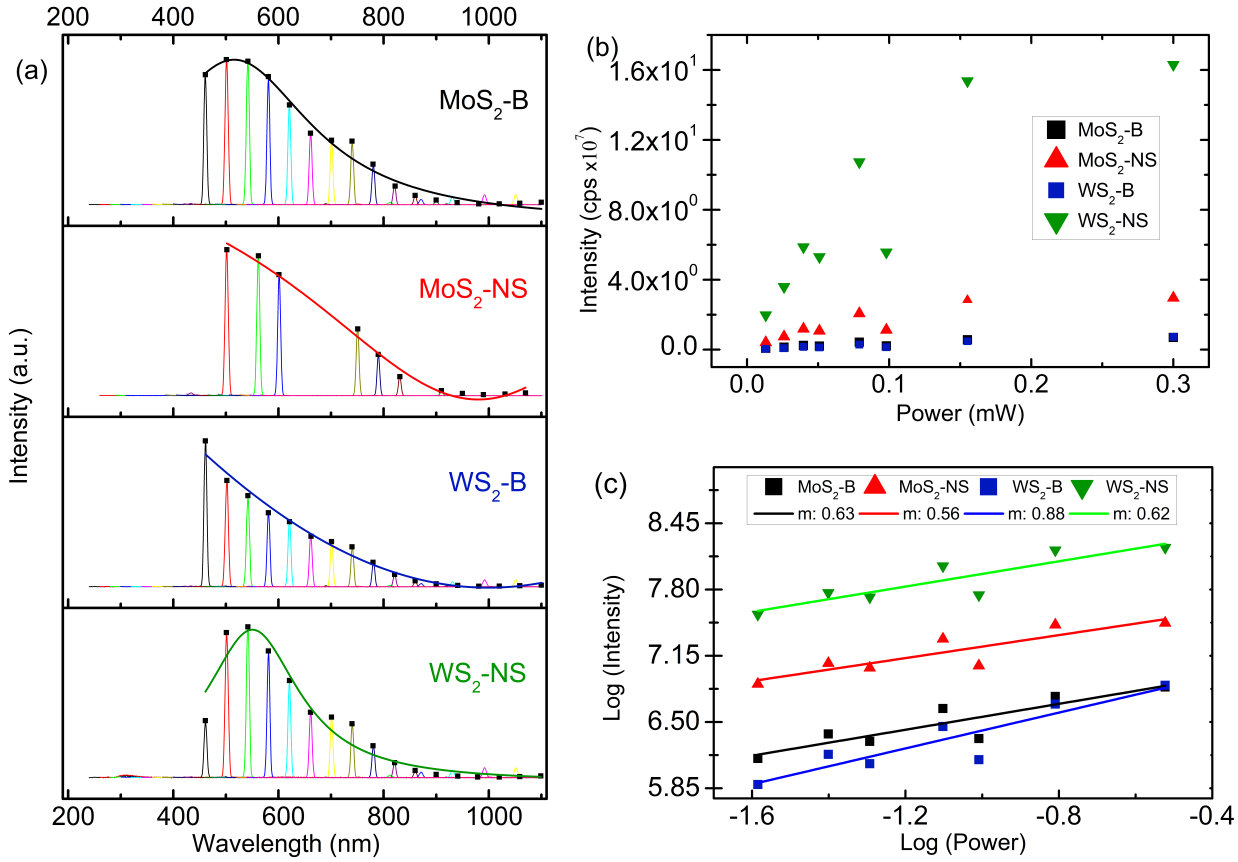

Figure S8: Fluorescence spectrum of suspensions of MoS_2 and WS_2 in bulk and exfoliated. (a) Half Harmonic generation response depending on the excited wavelength from 230nm to 550nm. The envelope wave shows a spectroscopic study of the "Exciton X". (b) Counts per second of Half Harmonic Generation peak at 780nm depending on the power of the incident light at λ=370nm. (c) Log of the intensity depending on power, the slope argue about the type of nonlinear optics behavior of the suspensions.

Best-solution results from large-scale SE

Table 2 summarizes best solution of ellipsometric analysis. In general, LPE samples adjust optically to the presence of only one type of flakes instead of a proportion of two types, depolarization factors N_x and N_y are lower than 1/3, d enter in a nanometric scale and surface coverages have the highest percentage related with void on LPE samples. To understand these results deeply, read SE methodology and results.

Table 2: Best solution results of island models on ellipsometric spectroscopy.

MoS_2			WS_2		
Parameter	Values	χ^2	Parameter	Values	χ^2
d [nm]	4.542	0.985	d [nm]	7.940	1.305
N_x=N_y	0.329		N_x=N_y	0.322	
N_z	0.342		N_z	0.356	
S_{void} [%]	75.37		S_{void} [%]	77.95	
$S_{1L-flakes}$ [%]	0.00		$S_{2L-flakes}$ [%]	0.00	
$S_{2L-flakes}$ [%]	24.63		$S_{3L-flakes}$ [%]	22.05	

References

(1) Castellanos, A.; Quereda, J.; van der Meulen, H. P.; Agrait, N.; Rubio-Bollinger, G. Spatially resolved optical absorption spectroscopy of single- and few-layer MoS_2 by hyperspectral imaging. *IOP, Nanotechnology* **2016**, *27*.

(2) Frisenda, R.; Niu, Y.; Gant, P.; Molina-Mendoza, A. J.; Schmidt, R.; Bratschitsch, R.; Liu, J.; Fu, L.; Dumcenco, D.; Kis, A.; Lara, D. P. D.; Castellanos-Gomez, A. Micro-reflectance and transmittance spectroscopy: a versatile and powerful tool to characterize 2D materials. *Journal of Physics D: Applied Physics* **2017**, *50*, 074002.

(3) Visic, B.; Dominko, R.; Gunde, M. K.; Hauptman, N.; Skapin, S. D.; Remskar, M. Optical properties of exfoliated MoS_2 coaxial nanotubes - analogues of graphene. *Nanoscale Research Letters* **2011**, *6*.

(4) Jia, G.; Zhang, Y.; Wang, P. Nano-photo-thermal energy drive MoS_2/ZnO nanoheterojunctions growing. *Opt. Mater. Express* **2016**, *6*, 876–883.

(5) Park, S.; Mutz, N.; Schultz, T.; Blumstengel, S.; Han, A.; Aljarb, A.; Li, L.-J.; List-Kratochvil, E. J. W.; Amsalem, P.; Koch, N. Direct determination of monolayer MoS_2 and WSe_2 exciton binding energies on insulating and metallic substrates. *2D Materials* **2018**, *5*, 025003.

(6) Zhu, B.; Chen, X.; Cui, X. Exciton Binding Energy of Monolayer WS_2. *Scientific Reports* **2015**, *5*, 9218.

(7) Bayat, A.; Saievar-Iranizad, E. Synthesis of blue photoluminescent WS_2 quantum dots via ultrasonic cavitation. *Journal of Luminescence* **2017**, *185*, 236–240.

(8) Pagona, G.; Bittencourt, C.; Arenal, R.; Tagmatarchis, N. Exfoliated semiconducting pure 2H-MoS_2 and 2H-WS_2 assisted by chlorosulfonic acid. *Chem. Commun.* **2015**, *51*, 12950–12953.